

# Multiple quantum criticality in a two-dimensional superconductor

J. Biscaras<sup>1</sup>, N. Bergeal<sup>1</sup>, S. Hurand<sup>1</sup>, C. Feuillet-Palma<sup>1</sup>, A. Rastogi<sup>2</sup>, R. C. Budhani<sup>2,3</sup>, M. Grilli<sup>4</sup>, S. Caprara<sup>4</sup> and J. Lesueur<sup>1\*</sup>

**The diverse phenomena associated with the two-dimensional electron gas (2DEG) that occurs at oxide interfaces include, among others, exceptional carrier mobilities, magnetism and superconductivity. Although these have mostly been the focus of interest for potential future applications, they also offer an opportunity for studying more fundamental quantum many-body effects. Here, we examine the magnetic-field-driven quantum phase transition that occurs in electrostatically gated superconducting LaTiO<sub>3</sub>/SrTiO<sub>3</sub> interfaces. Through a finite-size scaling analysis, we show that it belongs to the (2 + 1)D XY model universality class. The system can be described as a disordered array of superconducting puddles coupled by a 2DEG and, depending on its conductance, the observed critical behaviour is single (corresponding to the long-range phase coherence in the whole array) or double (one related to local phase coherence, the other one to the array). A phase diagram illustrating the dependence of the critical field on the 2DEG conductance is constructed, and shown to agree with theoretical proposals. Moreover, by retrieving the coherence-length critical exponent  $\nu$ , we show that the quantum critical behaviour can be clean or dirty according to the Harris criterion, depending on whether the phase-coherence length is smaller or larger than the size of the puddles.**

Two-dimensional electron gases at the interface between insulating oxides have raised considerable interest<sup>1–3</sup>. Indeed, they exhibit very high mobilities suitable for applications<sup>4</sup>, but also a rich phase diagram, with different quantum ground states such as magnetism<sup>5–8</sup> or superconductivity<sup>9,10</sup> for example. Moreover, these properties can be finely tuned using a gate voltage<sup>11,12</sup>. Therefore, 2DEGs at oxide interfaces are interesting systems to study quantum phase transitions (QPTs) that occur between different quantum states, when a parameter in the Hamiltonian crosses over a critical value<sup>13</sup>. The critical behaviour of the observables belongs to universality classes that depend on general properties of the system such as its dimensionality or its symmetries, and not on the microscopic details. The associated critical exponents obey specific rules, among which the so-called Harris criterion, which stipulates that the correlation-length exponent  $\nu$  must satisfy  $\nu \geq 2/d$  for dirty disordered systems, where  $d$  is the spatial dimensionality<sup>14</sup>.

An important example of a QPT is the transition from a superconducting to an insulating state in two dimensions, which has been a matter of debate for a long time. Numerous experiments with contrasting results have been performed, and a large variety of critical exponents have been found<sup>15</sup>. The nature of the non-superconducting state (metallic, insulator, localizing) and the role of the disorder are still unclear. The possibility that inhomogeneities spontaneously develop near the transition is a key issue to understanding the low-temperature phase diagram of these systems<sup>16–20</sup>, which may include multiple phase transitions. This is the issue we address in this Article.

Here we show that a perpendicular magnetic field applied to the superconducting 2DEG at the LaTiO<sub>3</sub>/SrTiO<sub>3</sub> interface drives

the system towards a weakly localizing metal. We evidence two critical behaviours corresponding to the dirty and clean limits of the Harris criterion, which can be controlled by the gate voltage. Indeed, finite-size scaling (FSS) analysis reveals that depending on the gate voltage and the temperature, the product of the critical exponents  $z\nu$  is  $2/3$  in some region of the phase diagram ( $z$  is the dynamical exponent), corresponding to the (2 + 1)D XY universality class in the clean regime<sup>13</sup>, and greater than 1 otherwise, as expected from the Harris criterion. We argue that these transitions correspond to the destruction of superconductivity by phase fluctuations in a disordered array of superconducting puddles coupled by a 2DEG. We propose a new phase diagram where intra- and inter-puddle physics come into play, and can be differently affected by two magnetic fields  $B_X$  and  $B_C$  ruling the phase decoherence inside or between the superconducting puddles respectively. We also provide quantitative evidence that the key parameter is the 2DEG conductance (as proposed in ref. 17), which determines whether the puddles can individually become superconducting (in this case  $B_X < B_C$ ) or not. In the latter case, superconductivity arises only from the puddle interplay and from their formation of a superconducting array, with  $B_X = B_C$ . This result demonstrates that the tunability of the superconducting 2DEG at the oxide interface is a powerful tool to study fundamental properties of superconductors in low dimensions. We anticipate that further insight into QPTs involving two-dimensional (2D) superconductors will emerge. For example, the role of disorder and inhomogeneity<sup>17,21–23</sup>, Coulomb repulsion, charge fluctuations and screening on the QPTs (refs 24,25) can be explored in more detail.

The LaTiO<sub>3</sub>/SrTiO<sub>3</sub> epitaxial interface exhibits a superconducting high-mobility 2DEG (ref. 10). We recently showed that  $T_c$  can be

<sup>1</sup>LPEM-UMR8213/CNRS-ESPCI ParisTech-UPMC, 10 rue Vauquelin, 75005 Paris, France, <sup>2</sup>Condensed Matter-Low Dimensional Systems Laboratory, Department of Physics, Indian Institute of Technology Kanpur, Kanpur 208016, India, <sup>3</sup>National Physical Laboratory, New Delhi 110012, India, <sup>4</sup>Istituto Nazionale per la Fisica della Materia, Unità di Roma 1 and SMC Center, and Dipartimento di Fisica Università di Roma 'La Sapienza', piazzale Aldo Moro 5, I-00185 Roma, Italy. \*e-mail: jerome.lesueur@espci.fr.

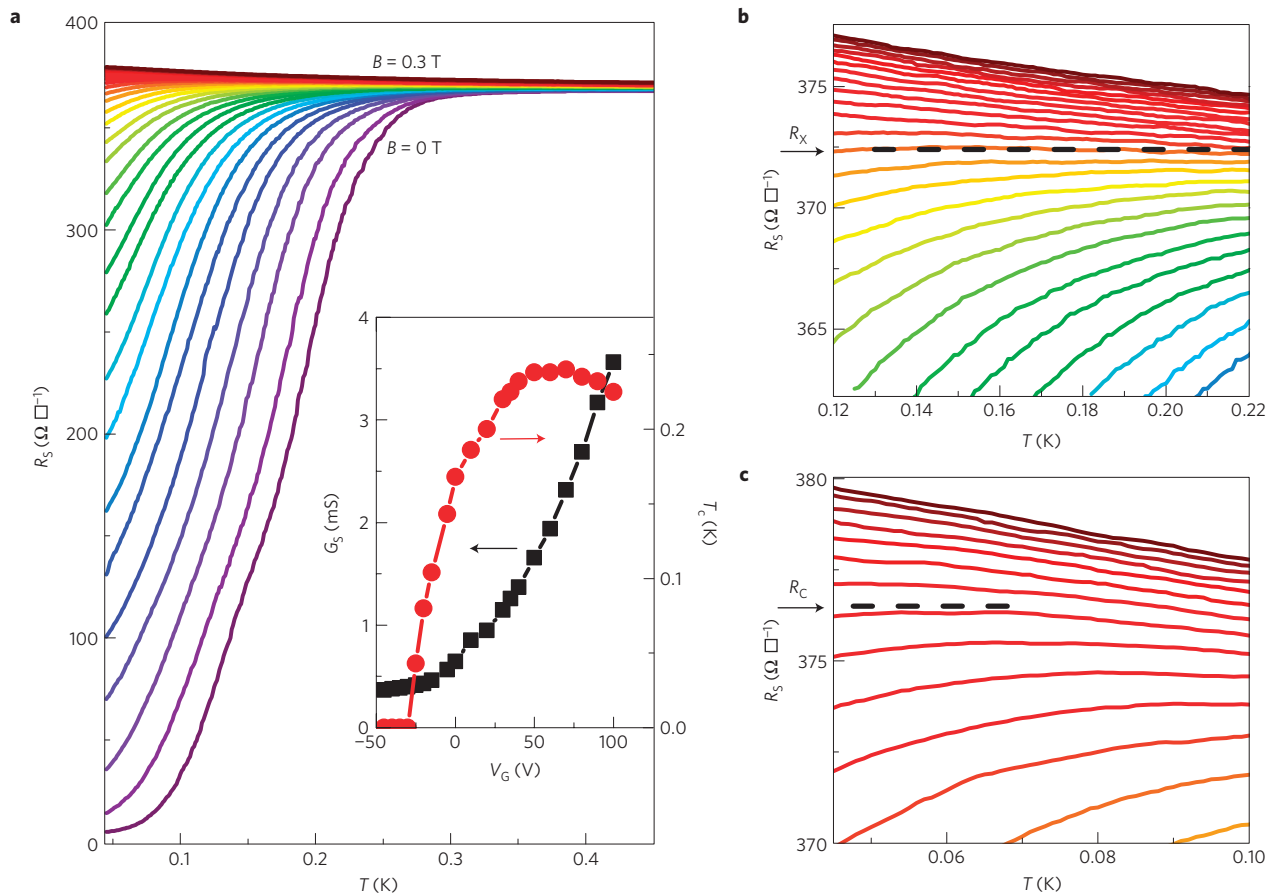


**Figure 1 | Superconductor-insulator transition induced by a magnetic field.** **a**, Sheet resistance  $R_S$  as a function of temperature for different magnetic fields from 0 to 0.3 T. Inset:  $T_c$  and  $G_S = 1/R_S$  as a function of the gate voltage  $V_G$ . **b**, Zoom on the same data showing the characteristic magnetic field  $B_X$ , for which  $R_S$  is constant between 0.12 and 0.22 K. **c**, Zoom on the same data showing the characteristic magnetic field  $B_C$ , which separates the two regimes at the lowest temperatures.

tuned by electrostatic gating from its maximum value of  $\sim 200$  mK to 0, and that superconductivity coincides with the presence of highly mobile carriers (HMCs) at the edge of the quantum well formed by the 2DEG at the interface<sup>12</sup>. It is therefore possible to prepare the system with a given  $T_c$  by controlling the gate voltage  $V_G$  (Fig. 1a, inset), and to study how the superconducting state is destroyed by a perpendicular magnetic field in this situation. Samples are grown by pulsed laser deposition of 15 unit cells of LaTiO<sub>3</sub> on TiO<sub>2</sub>-terminated (001) SrTiO<sub>3</sub> substrate (see ref. 10 for details). A metallic back gate is evaporated at the rear of the 500- $\mu\text{m}$ -thick SrTiO<sub>3</sub> substrate and connected to a voltage source ( $V_G$ ). Standard four-probe resistance measurements are made with a current sufficiently low to avoid any heating of the electrons at the lowest temperature. The polarization scheme described previously<sup>26</sup> is applied to ensure a reversible behaviour of the superconducting 2DEG.

The normal state exhibits the logarithmic temperature dependence of the conductivity characteristic of weak localization in two dimensions<sup>10</sup>. Magnetoresistance measurements beyond the superconducting critical field or above  $T_c$  can be analysed within the framework of the standard localization theory<sup>27</sup> for the whole range of parameters (magnetic field, temperature and gate voltage) used in this study<sup>28</sup>. Hence, the magnetic field turns the 2D superconductor into a 2D weakly localizing metal as shown in Fig. 1a for  $V_G = +80$  V, where the resistance per square  $R_S$  is plotted as a function of temperature  $T$  for different perpendicular magnetic fields  $B$ . A close-up view of the data reveals a critical field  $B_X$  that separates the two regimes, and for which

$R_S$  is constant (Fig. 1b). The same set of data plotted as  $R_S$  versus  $B$  for different temperatures in Fig. 2a exhibits a crossing point ( $R_X = 372.4 \Omega \square^{-1}$ ,  $B_X = 0.185$  T) where the resistivity does not depend on temperature. This is a first signature of a continuous QPT.

In such zero-temperature transitions, the ground state of the Hamiltonian is changed by an external parameter, such as the magnetic field for instance. Close to the transition the correlation length  $\xi$  in the space dimensions and the dynamical correlation length  $\xi_\tau$  in the imaginary time dimension of the quantum fluctuations diverge with a power-law dependence of the distance from the transition  $\delta = (B - B_X)$  (refs 13,15). At  $T = 0$  the correlation-length exponent  $\nu$  defined as  $\xi \propto |\delta|^{-\nu}$  and the dynamical scaling exponent  $z$  defined as  $\xi_\tau \propto \xi^z$  are believed to be independent of the microscopic details of the transition and depend on only a few properties of the system, such as the dimensionality and the range of the interactions, which define universality classes for the QPTs (ref. 13). The effective dimensionality of the system is  $d + z$ , where  $d$  is the spatial dimensionality. At finite temperature, the imaginary time dimension is limited by the temperature fluctuations so that the dimensionality of the system is  $d + z$  only at  $T = 0$ , and  $d$  at finite temperature<sup>15</sup>. More precisely, the finite temperature limits the size of the temporal direction by the thermal cutoff  $L_\tau = \hbar/k_B T$ , which is now an upper bound for the dynamical correlation length  $\xi_\tau$  near the critical point. It follows that in the spatial dimensions the quantum fluctuations lose phase coherence over a temperature-dependent dephasing length  $L_\phi \propto 1/T^{1/2}$  (ref. 13). This leads to

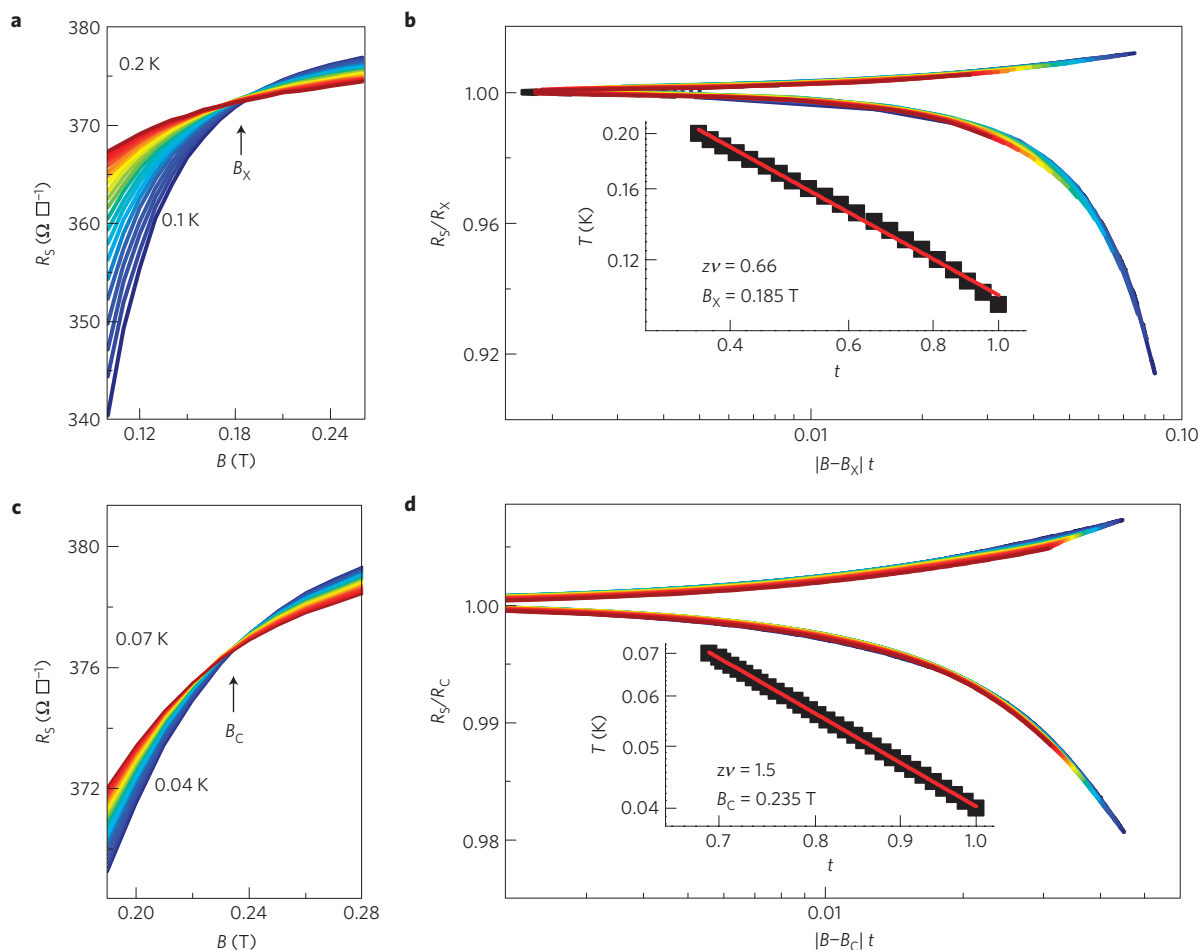


**Figure 2 | FSS analysis for  $V_G = +80$  V.** **a**, Sheet resistance  $R_S$  as a function of magnetic field  $B$  for different temperatures from 0.1 to 0.2 K. The crossing point is ( $B_X = 0.185$  T,  $R_X = 372.4 \Omega \square^{-1}$ ). **b**, FSS plot of  $R_S/R_X$  as a function of  $|B - B_X|t$  (see text for the definition of  $t$ ). Inset: temperature behaviour of the scaling parameter  $t$ . The power-law fit gives  $z\nu = 0.66$ . **c**,  $R_S$  as a function of  $B$  for different temperatures from 0.04 to 0.07 K. The crossing point is ( $B_C = 0.235$  T,  $R_C = 376.6 \Omega \square^{-1}$ ). **d**, FSS plot of  $R_S/R_C$  as a function of  $|B - B_C|t$ . Inset: temperature behaviour of the scaling parameter  $t$ . The power-law fit gives  $z\nu = 1.5$ .

a so-called FSS of the observables of the system. For instance, the resistance takes the form:

$$\frac{R_S}{R_X} = F\left(\frac{B - B_X}{T^{1/z\nu}}\right)$$

where  $F$  is an arbitrary function with  $F(0) = 1$  (ref. 29).

The critical exponents can then be retrieved by a scaling procedure as follows<sup>15</sup>. The resistance is rewritten as  $R_S(\delta, t) = R_X F(\delta t)$ , with  $t$  being an unknown parameter that depends only on  $T$ . The parameter  $t$  is then found at each temperature  $T$  by optimizing the collapse around the critical point between the curve  $R_S(\delta, t(T))$  at temperature  $T$  and the curve  $R_S(\delta, t(T_0))$  at the lowest temperature considered  $T_0$ , with  $t(T_0) = 1$ . The dependence of  $t$  with temperature should be a power law of the form  $t = (T/T_0)^{-1/z\nu}$  to have a physical sense, thus giving the critical exponent product  $z\nu$ . The interest of this procedure is to perform the scaling without knowing the critical exponent beforehand. The result of this procedure applied to the data in Fig. 1a shows that data collapse onto a single (bi-valued) curve in Fig. 2b, and yields  $z\nu = 0.66$  (Fig. 2b, inset).

In the literature,  $z\nu = 2/3$  has been observed for transitions driven by a perpendicular magnetic field in conventional 2D disordered superconductors such as a-NbSi (refs 30,31) or a-bismuth<sup>15,32</sup>. The exponent  $\nu \sim 2/3$  corresponds to the clean 3D XY

universality class according to series expansion calculations<sup>33,34</sup> or numerical simulations<sup>35,36</sup>. This also corresponds to a (2 + 1)D XY for a 2D superconductor, where the extra dimension refers to the imaginary time in the quantum transition, provided the dynamical exponent  $z$  is set to 1 (refs 13,29). In that case, long-range superconducting correlations are destroyed by quantum phase fluctuations. In general, the dynamical exponent  $z$  is found to be 1, corresponding to long-range Coulomb interaction between charges<sup>13,29</sup>, as has been measured in a-MoGe for instance<sup>37</sup>. In the absence of a specific screening or dissipation mechanism<sup>38</sup>, there is no reason to invoke short-range interactions, which would set  $z \neq 1$ , but this remains to be experimentally proved. Therefore, if  $z = 1$ , then  $\nu = 2/3$ , which means that  $\nu \leq 2/d$ , with the spatial dimension  $d = 2$ . According to the very general Harris criterion<sup>14</sup>, the system is in the clean limit at the relevant scale for the transition, namely the dephasing length  $L_\phi$ . In 2D disordered systems, that is, in the dirty regime,  $\nu$  is expected to increase beyond 1 (ref. 36), following the Harris criterion, as observed in a-MoGe (ref. 37), InOx (ref. 39), ultrathin high- $T_c$  superconductors<sup>40</sup> or more recently in graphene-metal hybrids<sup>41</sup> for instance.

We now focus on the same  $R_S$  versus  $T$  curves below 0.1 K ( $V_G = +80$  V). A close-up view in Fig. 1c evidences another critical field  $B_C$  for which the resistance is constant in a restricted range of temperature and  $\partial R/\partial T$  changes sign. Reported in Fig. 2c,  $R_S$  versus  $B$  curves exhibit a crossing point ( $B_C = 0.235$  T,  $R_C = 376.6 \Omega \square^{-1}$ ),

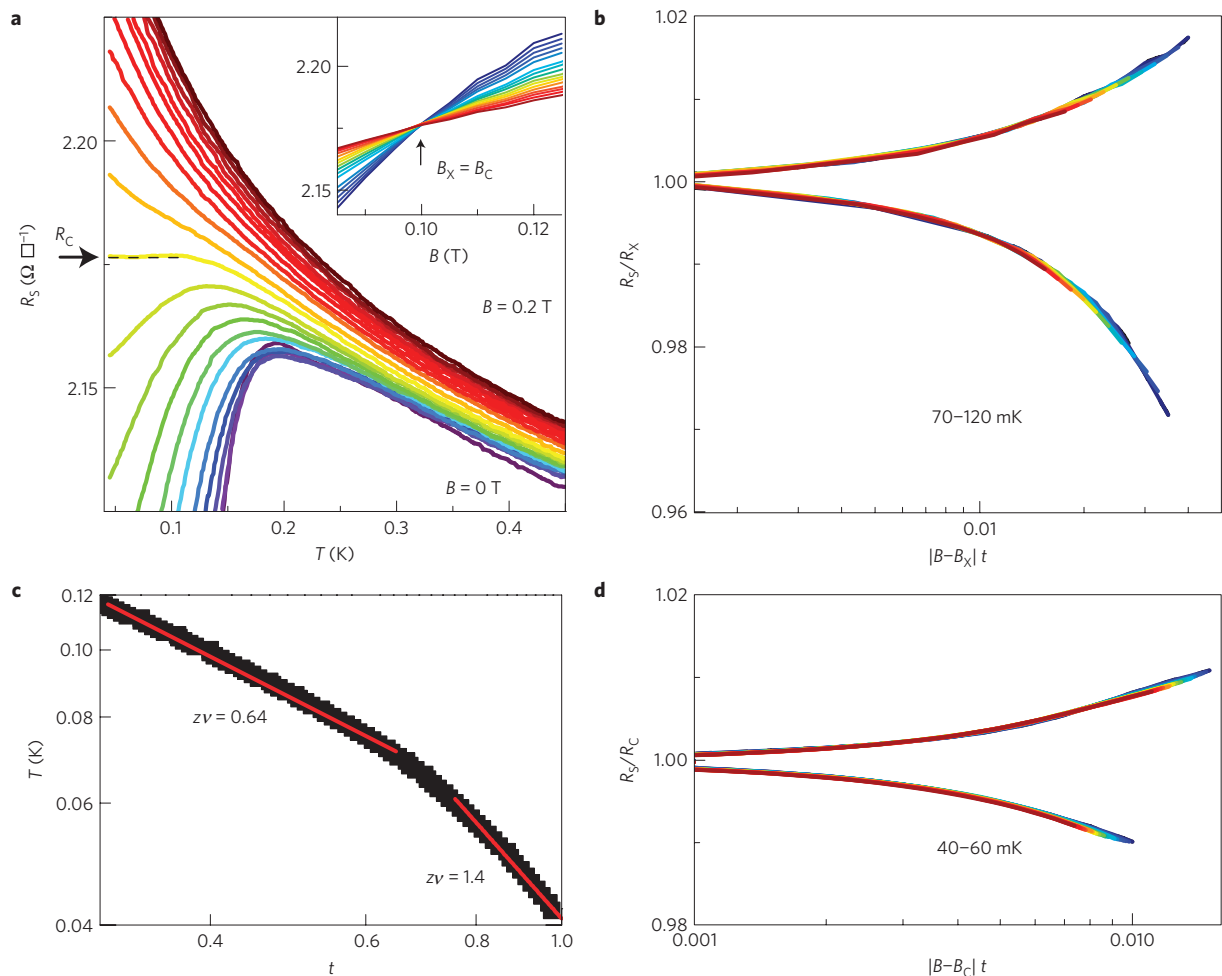


**Figure 3** | FSS for  $V_G = -15$  V. **a**, Sheet resistance  $R_S$  as a function of temperature for different magnetic fields from 0 to 0.2 T. Inset: corresponding  $R_S$  as a function of the magnetic field for different temperatures from 0.07 to 0.12 K. The crossing point is ( $B_X = 0.1$  T,  $R_X = 2,176 \Omega \square^{-1}$ ). **b**, Temperature behaviour of the scaling parameter  $t$ : two distinct slopes are evidenced, 0.64 at high temperature and 1.4 at low temperature. **c**, FSS plot of  $R_S/R_X$  as a function of  $|B - B_X|t$  corresponding to the high-temperature regime, with  $z\nu = 0.64$ . **d**, FSS plot of  $R_S/R_C$  as a function of  $|B - B_C|t$  corresponding to the low-temperature regime, with  $z\nu = 1.4$ .

and the FSS analysis shows a good collapse of the curves, leading to a critical exponent product  $z\nu \sim 1.5$  (Fig. 2d). This is clearly greater than 1. The system is in the dirty limit of the Harris criterion at the scale  $L_\phi$ .

As a conclusion for  $V_G = +80$  V, the system seems to exhibit a clean critical behaviour ( $z\nu \sim 2/3$ ) that can be seen between 120 and 220 mK, and a dirty one ( $z\nu \sim 3/2$ ) at lower temperature. At first sight, this is contradictory because the finite-temperature scaling behaviour of a QPT is expected to hold down to the lowest temperatures. It was already noticed<sup>19,42</sup> that FSS can be performed in 2D superconductors under a magnetic field in a restricted range of finite temperatures. These authors argued that this can be understood if the low-temperature phase is inhomogeneous. We will come back to this point later on.

When the gate voltage is tuned to lower or even negative values, the system is driven towards a more resistive state, and  $T_c$  decreases (Fig. 1a, inset). In Fig. 3a,  $R_S$  is shown as a function of the temperature for different magnetic fields and for a gate voltage  $V_G = -15$  V. A plateau is clearly seen down to the lowest temperature for a critical field  $B_X = 0.1$  T ( $R_X = 2176 \Omega \square^{-1}$ ), as confirmed by the presence of a crossing point (Fig. 3a, inset). The FSS analysis reveals that two regimes take place as shown in Fig. 3b. Indeed, two distinct  $z\nu$  values can be extracted: at high temperature (70–120 mK)  $z\nu \sim 2/3$  and at the lowest temperatures  $z\nu \sim 3/2$ . The

corresponding collapses of the data depicted in Fig. 3c,d confirm the existence of the quantum critical behaviour.

We made the same analysis for all of the gate voltages between  $V_G = -40$  V and  $V_G = +100$  V. The results are shown in Fig. 4. For  $V_G \geq +10$  V, two distinct critical fields  $B_X$  and  $B_C$  ( $B_C > B_X$ ) can be found (Fig. 4a, region II), whereas for  $V_G \leq +10$  V, they merge into a unique value (region I). Two important observations need to be made:  $B_X$  increases with  $V_G$  and then saturates when  $B_X \neq B_C$  to a value  $B_d$ ;  $B_C$  matches  $T_c$  defined as the temperature where the normal-state resistance drops by 10% (ref. 12).  $B_C$  is therefore the critical field that fully destroys superconductivity in the system. The critical exponent products  $z\nu$  extracted from the FSS analysis around both critical fields are reported as a function of  $V_G$  in Fig. 4b.  $z\nu$  corresponding to  $B_X$  is constant and equals  $\sim 2/3$ : the quantum critical behaviour is in the (2 + 1)D XY clean limit. For  $B_C$ ,  $z\nu$  changes with  $V_G$ , with rather important error bars due to the finite scaling range in temperature, but is always larger than 1, indicating that the QPT is in the dirty limit.

To account for these observations, we propose the following scenario based on the XY model where superconductivity is destroyed by phase fluctuations in a 2D superconductor. We suppose that the system consists of superconducting islands coupled by non-superconducting metallic regions (see Fig. 5 for a sketch). Indeed, as shown previously<sup>12</sup>, the superconducting 2DEG is made

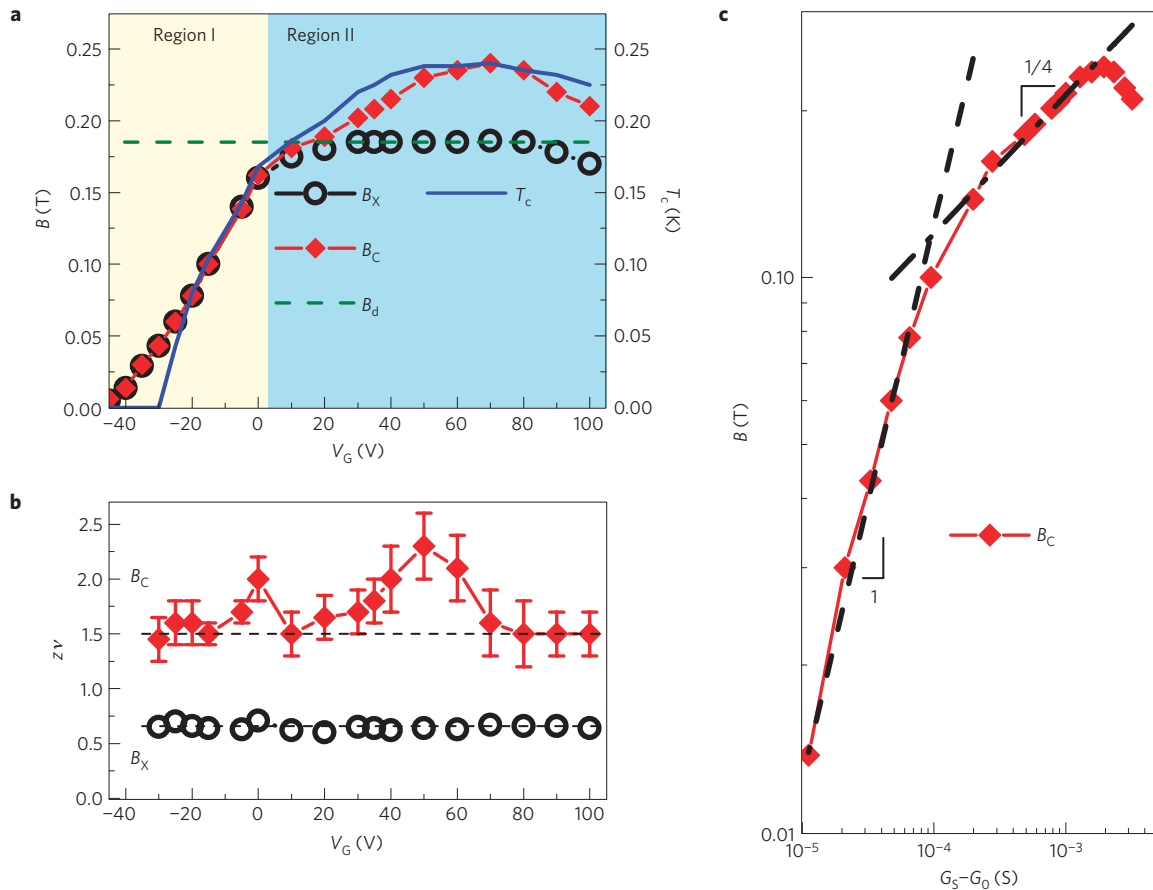


**Figure 4 | The two quantum critical behaviours.** **a**,  $B_X$ ,  $B_C$  (left scale) and  $T_c$  (right scale) as a function of  $V_G$ . The dashed line corresponds to  $B_d$  (see text). Regions I and II refers to the low, and respectively high, coupling regimes (see text). **b**,  $\nu$  as a function of  $V_G$  for the two transitions (when  $B_X = B_C$ ,  $B_C$  has been assigned to the low-temperature regime, and  $B_X$  to the high-temperature one).  $\nu = 0.66$  is constant for the high-temperature transition (error bars are smaller than the size of the circle symbols).  $\nu$  is between 1.5 and 2.3 for the dirty one. The dashed lines correspond to  $\nu = 2/3$  and  $\nu = 3/2$ . **c**,  $B_C$  as a function of  $G_S$  on a log scale ( $G_0 = 356 \mu\text{S}$  is the conductance at  $V_G = -45 \text{ V}$ , where  $B_C$  goes to 0). Dashed lines have slopes 1 and 1/4 respectively as expected from the model of ref. 17.

of two types of carrier, a few HMCs and a majority of low mobile carriers. We argued that the presence of HMCs triggers superconductivity in the system. The density of HMCs (ref. 12; in the  $10^{12} \text{ cm}^{-2}$  range) and its evolution with the gate voltage is very similar to the superfluid density directly measured in ref. 43 in  $\text{LaAlO}_3/\text{SrTiO}_3$  interfaces. We therefore assume that HMCs form the superfluid with intrinsic inhomogeneity due to its very low average density and the associated density fluctuations, and that low mobile carriers form the metal that provides long-range coupling. The system is therefore described as a disordered array of superconducting puddles of size  $L_d$  coupled by a metallic 2DEG. Such a situation has been studied previously<sup>17</sup>. Superconducting phase coherence is governed by the transport properties of the metallic part through the proximity effect, and depends on the 2DEG conductance  $G_{2\text{DEG}}$ . If the coupling is strong enough (high  $G_{2\text{DEG}}$ ), puddles can develop full local superconductivity and two critical behaviours can be observed corresponding respectively to the puddles themselves and to the disordered array of puddles. In the opposite case (low  $G_{2\text{DEG}}$ ), decoupled puddles are always in a fluctuating regime, and only the full array transition can be seen at low temperature. These two regimes can be observed in  $\text{LaTiO}_3/\text{SrTiO}_3$  interfaces, and the transition from one to the other can be controlled by the gate voltage. Indeed, the conductance  $G_S = 1/R_S$  increases with  $V_G$  (Fig. 1a, inset), and so does the coupling. Region I is therefore the low coupling regime with a single transition ( $B_X = B_C$ ), whereas region II refers to the

high coupling one with two transitions ( $B_C > B_X$ ). In the latter case,  $B_X$  is the critical field for the puddle transition and  $B_C$  the one for the whole array: as a consequence  $T_c$  scales with  $B_C$  as observed experimentally.

The model described in ref. 17 develops a full analysis of the long-range coupling between puddles. It introduces the concept of an optimal puddle<sup>17</sup> to account for the statistical distribution of puddle sizes, and shows that the critical magnetic field  $B_C$  scales with the coupling parameter  $G_{2\text{DEG}}$ . At low conductance,  $B_C \propto G_{2\text{DEG}}$ , whereas at high conductance,  $B_C \propto G_{2\text{DEG}}^{1/4}$ . To test the model in more detail, we plotted the critical field  $B_C$  as a function of the conductance  $G_S$  on a log-scale in Fig. 4c. The data are in good agreement with the theory. Not only can the two regimes be clearly identified, but also the values of the slopes correspond to the calculated one. This is a strong indication that the model of ref. 17 is a good representation of the physics involved in these experiments.

On this basis, we can now analyse the QPT, remembering that the thermal dephasing length behaves as  $L_\phi \sim T^{-1/z}$  ( $z = 1$  here). A schematic illustrating the situation is shown in Fig. 5a. Let us first focus on region II as defined in Fig. 4. At high temperature, the phase dephasing length  $L_\phi$  is smaller than the superconducting puddle size  $L_d$ , and the intra-puddle physics dominates. The critical field  $B_X$  corresponds to the dephasing field  $B_d$  on a puddle of size  $L_d$  ( $B_d \sim \Phi_0/L_d^2$ , where  $\Phi_0$  is the flux quantum)<sup>17,18</sup>, and does not depend on the microscopic parameters of the system tuned by  $V_G$ . This is why it is constant as a function of  $V_G$  ( $B_X = B_d$ )

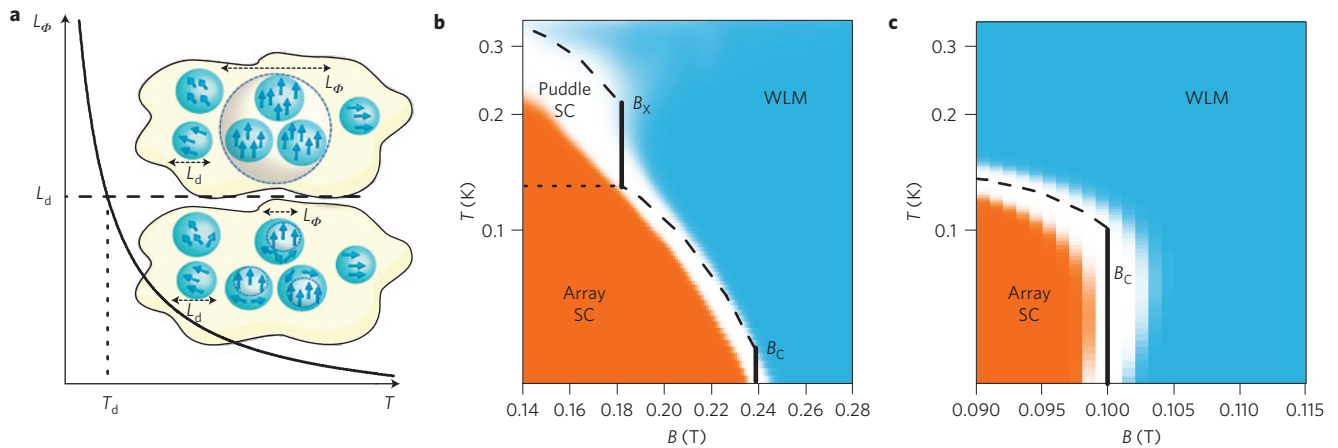


**Figure 5 | Sketch of the role of mesoscopic disorder on the QPT and phase diagrams.** **a**, The dephasing length  $L_\phi$  diverges with decreasing temperature, and reaches the size of the superconducting puddles  $L_d$  at  $T_d$ . The insets show a piece of material in the two regimes. At high temperature (bottom),  $L_\phi < L_d$  and the system is in the clean limit, whereas at low temperature (top),  $L_\phi > L_d$ , and the system is in the dirty limit. In this drawing, superconducting puddles (blue) are coupled through a 2DEG (yellow). The arrows symbolize the local phase of the superconductor. **b**, Phase diagram in the  $B$ - $T$  plane for  $V_G = +80$  V. The derivative  $\partial R/\partial T$  is plotted as a colour scale (blue for negative values, orange for positive ones and white around 0), as a function of the magnetic field  $B$  and the temperature  $T$  (log scale). The two critical fields  $B_X$  and  $B_C$  are reported, together with the different phases: WLM refers to weakly localizing metal, puddle SC to the region where complete superconductivity within the puddles can be observed, array SC where the whole array is superconducting. **c**, Phase diagram in the  $B$ - $T$  plane for  $V_G = -15$  V. A single critical field  $B_C$  is observed corresponding to the transition of the whole array.

as shown in Fig. 4a. From the value of  $B_d$ , we can estimate  $L_d$  to be of the order of 100 nm. As  $L_\phi < L_d$ , the system is in the clean limit, and  $z\nu \sim 2/3 < 1$  (Fig. 4b). When lowering the temperature,  $L_\phi$  crosses  $L_d$  at  $T_d$ , and the whole array undergoes the transition with a critical field  $B_C$ . In that case, phase fluctuations extend over wide disordered regions and the dirty (2+1)D XY model applies as expected from the Harris criterion ( $z\nu > 1$  as shown in Fig. 4b). In region I, only the array exhibits a transition with a single critical field  $B_C$ . However, as the temperature is lowered,  $L_\phi$  also crosses  $L_d$ , and we therefore observe a transition from a clean ( $z\nu < 1$ ) to a dirty ( $z\nu > 1$ ) (2+1)D XY limit. At this point, it is worthwhile mentioning that, strictly speaking, the transition at  $B_C$  is the only true QPT, because the scaling holds down to the lowest temperature. However, at sufficiently high temperature, the transition at  $B_X$  exhibits fluctuations corresponding also to a real QPT that is never reached. Indeed, the diverging dephasing length crosses  $L_d$ , which acts as a cutoff length for the intra-puddle physics.  $B_X$  is therefore a crossover field<sup>17</sup> marking the change of quantum critical behaviour.

Such an analysis reveals that the tunable LaTiO<sub>3</sub>/SrTiO<sub>3</sub> epitaxial interface is a unique system to study the superconducting QPT in two dimensions, which is well described by the (2+1)D XY model as expected. The role of disorder on the critical exponents is clearly evidenced, together with the possibility of observing multiple phase transitions as previously proposed theoretically<sup>16–18</sup>.

Our study sheds light on the critical role of superfluid density fluctuations and intrinsic inhomogeneities when approaching the phase transition. A traditional view of the QPT in 2D superconductors is based on the so-called fermionic scenario<sup>44</sup>, where superconductivity disappears because Cooper pairs are destroyed, as opposed to the dirty boson scenario<sup>29</sup>, where they localize and form an insulator. In the latter case, phase fluctuations dominate and the QPT takes place for critical resistances  $R_C$  close to the quantum resistance  $R_Q = h/4e^2 \simeq 6.5 \text{ k}\Omega \square^{-1}$  and  $\nu > 1$ . Experiments reveal that the situation is more complex<sup>15</sup>, in particular when inhomogeneities play a role<sup>19</sup>. Ref. 39 compiled experimental results in the literature and clearly evidenced two behaviours: the QPT separates a superconducting phase from a weakly localizing metal in the less disordered systems ( $R_C \leq R_Q$ ), and from an insulator in strongly disordered materials ( $R_C \sim R_Q$ ). Our data ( $0.04 \leq R_C/R_Q \leq 0.4$ ) fully agree with this picture,

and the non-superconducting phase is indeed always a weakly localizing metal. New theoretical scenarios emerged<sup>16–18</sup> based on superconducting puddles in a 2D metal, where phase fluctuations play a crucial role (the XY model applies), compatible with critical resistances lower than  $R_Q$ , and leading to new phase diagrams. Our results show the relevance of this approach. Moreover, we evidence that the phase diagram is not universal, because it can be changed by the gate voltage, as shown in Fig. 5b,c, which presents the  $B$ - $T$  phase diagrams corresponding to  $V_G = +80$  V and  $V_G = -15$  V, respectively. In contrast, the critical exponent for high-temperature scaling  $\nu \sim 2/3$  always corresponds to the clean (2+1)D XY, showing that the transition is driven by phase fluctuations in a 2D superconductor. The low-temperature value of  $\nu$  is always greater than 1, indicating that disorder ultimately controls the QPT. If its value is close to  $z\nu = 3/2$  in most of the phase diagram, the limited range of temperature for the FFS analysis prevents one from drawing strong conclusions. One cannot exclude that the universality class refers to classical percolation ( $\nu = 4/3$ ) between superconducting puddles. Quantum percolation ( $\nu = 7/3$ ) could also take place in some part of the phase diagram (see ref. 39 for a discussion on this point for example). More work is needed to clarify this important point.

We have showed that the superconducting 2DEG at the LaTiO<sub>3</sub>/SrTiO<sub>3</sub> interface undergoes a QPT from a superconductor to a weakly localizing metal on applying a perpendicular magnetic field, driven by phase fluctuations and well described by the (2+1)D XY model, as expected. By tuning the gate voltage, it is possible to explore the clean and dirty regimes according to the Harris criterion, with a critical exponents product  $z\nu = 2/3$  in the former case, in agreement with previous evaluations in the parent system LaAlO<sub>3</sub>/SrTiO<sub>3</sub> (refs 11,45), and greater than 1 otherwise. The system is well described by a disordered array of superconducting puddles coupled by a 2DEG, which can exhibit two critical behaviours, one related to regional or local ordering, and another one corresponding to long-range phase coherence, as proposed theoretically<sup>16–18</sup>. The key parameter, that is, the coupling constant (the 2DEG conductance), can be tuned at will to explore the phase diagram of the system. This is important in the context of recent studies of strongly disordered 2D superconductors where intrinsic inhomogeneities appear at mesoscopic scales<sup>17,46,47</sup>, with

coexistence of superconducting and non-superconducting regions. Recent work on artificial ordered metallic networks addresses this issue<sup>48</sup>, but does not reach the insulating state. Our study opens the way for exploring the physics of disordered superconductors, and beyond, the more general problem of phase coherence in multiscale systems such as strongly correlated materials that are phase-separated<sup>49</sup> or spin-textured<sup>50</sup>.

Received 23 October 2012; accepted 6 March 2013;  
published online 14 April 2013

## References

- Mannhart, J. & Schlom, D. G. Oxide interfaces—an opportunity for electronics. *Science* **327**, 1607–1611 (2010).
- Mannhart, J., Blank, D. H. A., Hwang, H. Y., Millis, A. J. & Triscone, J. M. Two-dimensional electron gases at oxide interfaces. *Mater. Res. Soc. Bull.* **33**, 1027–1034 (2008).
- Hwang, H. Y. *et al.* Emergent phenomena at oxide interfaces. *Nature Mater.* **11**, 103–113 (2012).
- Ohtomo, A. & Hwang, H. Y. A high-mobility electron gas at the LaAlO<sub>3</sub>/SrTiO<sub>3</sub> heterointerface. *Nature* **427**, 423–426 (2004).
- Brinkman, A. *et al.* Magnetic effects at the interface between non-magnetic oxides. *Nature Mater.* **6**, 493–496 (2007).
- Shalom, M. B. *et al.* Anisotropic magnetotransport at the SrTiO<sub>3</sub>/LaAlO<sub>3</sub> interface. *Phys. Rev. B* **80**, 140403 (2009).
- Bert, J. A. *et al.* Direct imaging of the coexistence of ferromagnetism and superconductivity at the LaAlO<sub>3</sub>/SrTiO<sub>3</sub> interface. *Nature Phys.* **7**, 767–771 (2011).
- Li, L., Richter, C., Mannhart, J. & Ashoori, R. C. Coexistence of magnetic order and two-dimensional superconductivity at LaAlO<sub>3</sub>/SrTiO<sub>3</sub> interfaces. *Nature Phys.* **7**, 762–766 (2011).
- Reyren, N. *et al.* Superconducting interfaces between insulating oxides. *Science* **317**, 1196–1199 (2007).
- Biscaras, J. *et al.* Two-dimensional superconductivity at a Mott insulator/band insulator interface LaTiO<sub>3</sub>/SrTiO<sub>3</sub>. *Nature Commun.* **1**, 89 (2010).
- Cavaglia, A., Gariglio, S., Reyren, N. & Jaccard, D. Electric field control of the LaAlO<sub>3</sub>/SrTiO<sub>3</sub> interface ground state. *Nature* **456**, 624–627 (2008).
- Biscaras, J. *et al.* Two-dimensional superconducting phase in LaTiO<sub>3</sub>/SrTiO<sub>3</sub> heterostructures induced by high-mobility carrier doping. *Phys. Rev. Lett.* **108**, 247004 (2012).
- Sondhi, S. L., Girvin, S. M., Carini, J. P. & Shahar, D. Continuous quantum phase transitions. *Rev. Mod. Phys.* **69**, 315–333 (1997).
- Harris, H. B. Effect of random defects on the critical behaviour of Ising models. *J. Phys. C* **7**, 1671–1692 (1974).
- Goldman, A. M. Superconductor–insulator transitions. *Int. J. Mod. Phys. B* **24**, 4081–4101 (2010).
- Spivak, B., Zyuzin, A. & Hruska, M. Quantum superconductor–metal transition. *Phys. Rev. B* **64**, 132502 (2001).
- Spivak, B., Oretto, P. & Kivelson, S. Theory of quantum metal to superconductor transitions in highly conducting systems. *Phys. Rev. B* **77**, 214523 (2008).
- Feigel'man, M. V., Larkin, A. I. & Skvortsov, M. A. Quantum superconductor–metal transition in a proximity array. *Phys. Rev. Lett.* **86**, 1869–1872 (2001).
- Mason, N. & Kapitulnik, A. True superconductivity in a two-dimensional superconducting–insulating system. *Phys. Rev. B* **64**, 060504 (2001).
- Shimshoni, E., Auerbach, A. & Kapitulnik, A. Transport through quantum melts. *Phys. Rev. Lett.* **80**, 3352–3355 (1998).
- Caprara, S., Peronaci, F. & Grilli, M. Intrinsic instability of electronic interfaces with strong Rashba coupling. *Phys. Rev. Lett.* **109**, 196401 (2012).
- Bucheli, D., Caprara, S., Castellani, C. & Grilli, M. Metal–superconductor transition in low-dimensional superconducting clusters embedded in two-dimensional electron systems. *New J. Phys.* **15**, 023014 (2013).
- Caprara, S., Grilli, M., Benfatto, L. & Castellani, C. Effective medium theory for superconducting layers: A systematic analysis including space correlation effects. *Phys. Rev. B* **84**, 014514 (2011).
- Goldman, A. M. & Marković, N. Superconductor–insulator transitions in the two-dimensional limit. *Phys. Today* **51**, 39 (November, 1998).
- Kapitulnik, A., Mason, N., Kivelson, S. A. & Chakravarty, S. Effects of dissipation on quantum phase transitions. *Phys. Rev. B* **63**, 125322 (2001).
- Biscaras, J. *et al.* Irreversibility and time relaxation in electrostatic doping of oxide interfaces. Preprint at <http://arxiv.org/abs/1206.1198> (2012).
- Maekawa, S. & Fukuyama, H. Magnetoresistance in two-dimensional disordered systems. Effects of Zeeman splitting and spin–orbit scattering. *J. Phys. Soc. Jpn* **50**, 2516–2524 (1981).
- Biscaras, J. *Two-dimensional superconductivity at titanium oxide interfaces* PhD thesis (2012).
- Fisher, M. P. A. Quantum phase transitions in disordered two-dimensional superconductors. *Phys. Rev. Lett.* **65**, 923–926 (1990).
- Aubin, H. *et al.* Magnetic-field-induced quantum superconductor–insulator transition in Nb<sub>0.15</sub>Si<sub>0.85</sub>. *Phys. Rev. B* **73**, 094521 (2006).
- Marrache-Kikuchi, C. *et al.* Thickness-tuned superconductor–insulator transitions under magnetic field in a-NbSi. *Phys. Rev. B* **78**, 144520 (2008).
- Marković, N., Christiansen, C. & Goldman, A. Thickness-magnetic field phase diagram at the superconductor–insulator transition in 2D. *Phys. Rev. Lett.* **81**, 5217–5220 (1998).
- Jasnow, D. & Wortis, M. High-temperature critical indices for the classical anisotropic Heisenberg model. *Phys. Rev.* **176**, 739–750 (1968).
- Wilson, K. & Fisher, M. Critical exponents in 3.99 dimensions. *Phys. Rev. Lett.* **28**, 240–243 (1972).
- Li, Y. H. & Teitel, S. Finite-size scaling study of the 3-dimensional classical XY model. *Phys. Rev. B* **40**, 9122–9125 (1989).
- Kisker, J. & Rieger, H. Bose-glass and Mott-insulator phase in the disordered boson Hubbard model. *Phys. Rev. B* **55**, R11981–R11984 (1997).
- Yazdani, A. & Kapitulnik, A. Superconducting–insulating transition in two-dimensional a-MoGe thin films. *Phys. Rev. Lett.* **74**, 3037–3040 (1995).
- Mason, N. & Kapitulnik, A. Superconductor–insulator transition in a capacitively coupled dissipative environment. *Phys. Rev. B* **65**, 220505 (2002).
- Steiner, M. A., Breznay, N. P. & Kapitulnik, A. Approach to a superconductor-to-Bose-insulator transition in disordered films. *Phys. Rev. B* **77**, 212501 (2008).
- Bollinger, A. T. *et al.* Superconductor–insulator transition in La<sub>2–x</sub>Sr<sub>x</sub>CuO<sub>4</sub> at the pair quantum resistance. *Nature* **472**, 458–460 (2011).
- Allain, A., Han, Z. & Bouchiat, V. Electrical control of the superconducting-to-insulating transition in graphene-metal hybrids. *Nature Mater.* **11**, 590–594 (2012).
- Mason, N. & Kapitulnik, A. Dissipation effects on the superconductor–insulator transition in 2D superconductors. *Phys. Rev. Lett.* **82**, 5341–5344 (1999).
- Bert, J. A. *et al.* Gate-tuned superfluid density at the superconducting LaAlO<sub>3</sub>/SrTiO<sub>3</sub> interface. *Phys. Rev. B* **86**, 060503 (2012).
- Finkel'shtein, A. M. Superconducting transition temperature in amorphous films. *JETP Lett.* **45**, 46–49 (1987).
- Schneider, T., Cavaglia, A. D., Gariglio, S., Reyren, N. & Triscone, J. M. Electrostatically-tuned superconductor–metal–insulator quantum transition at the LaAlO<sub>3</sub>/SrTiO<sub>3</sub> interface. *Phys. Rev. B* **79**, 184502 (2009).
- Sacépé, B. *et al.* Localization of preformed Cooper pairs in disordered superconductors. *Nature Phys.* **7**, 239–244 (2011).
- Bouadim, K., Loh, Y. L., Randeria, M. & Trivedi, N. Single- and two-particle energy gaps across the disorder-driven superconductor–insulator transition. *Nature Phys.* **7**, 884–889 (2011).
- Eley, S., Gopalakrishnan, S., Goldbart, P. M. & Mason, N. Approaching zero-temperature metallic states in mesoscopic superconductor-normal-superconductor arrays. *Nature Phys.* **8**, 59–62 (2011).
- Dagotto, E. Complexity in strongly correlated electronic systems. *Science* **309**, 257–262 (2005).
- Ruben, G., Morgan, M. & Paganin, D. Texture control in a pseudospin Bose–Einstein condensate. *Phys. Rev. Lett.* **105**, 220402 (2010).

## Acknowledgements

The authors thank C. Di Castro, C. Castellani, L. Benfatto and C. Kikuchi-Marrache for stimulating discussions. This work has been supported by the Région Île-de-France in the framework of CNano IdF and Sesame programmes. Research in India was funded by the Department of Information Technology, Government of India.

## Author contributions

A.R. and R.C.B. prepared the samples. J.B. and S.H. performed the measurements assisted by N.B. J.B., N.B., C.F.-P., M.G., S.C. and J.L. carried out the analysis of the results and wrote the article.

## Additional information

Reprints and permissions information is available online at [www.nature.com/reprints](http://www.nature.com/reprints). Correspondence and requests for materials should be addressed to J.L.

## Competing financial interests

The authors declare no competing financial interests.